Catalysis Communications 40 (2013) 51–54

Contents lists available at SciVerse ScienceDirect

Catalysis Communications

journal homepage: www.elsevier.com/locate/catcom

Short Communication

A novel noble metal-free ZnS–WS_2/CdS composite photocatalyst for H_2 evolution under visible light irradiation

Guoping Chen [a,b], Fan Li [a,b], Yuzun Fan [c], Yanhong Luo [a,b], Dongmei Li [a,b,]*, Qingbo Meng [a,b,]**

[a] Key Laboratory for Renewable Energy, Institute of Physics, Chinese Academy of Sciences, Beijing 100190, PR China
[b] Beijing Key Laboratory for New Energy Materials and Devices, Institute of Physics, Chinese Academy of Sciences, Beijing 100190, PR China
[c] Key Laboratory of Bio-Inspired Smart Interfacial Science and Technology of Ministry of Education, School of Chemistry and Environment, Beihang University, Beijing 100191, PR China

ARTICLE INFO

Article history:
Received 12 April 2013
Received in revised form 23 May 2013
Accepted 24 May 2013
Available online 4 June 2013

Keywords:
ZnS–WS_2/CdS
H_2 evolution
Synergistic effect
ZnS passivation
Noble metal-free

ABSTRACT

A novel ZnS–WS_2/CdS composite photocatalyst for H_2 evolution under visible light irradiation has been successfully synthesized. The loading amounts of WS_2 and ZnS on the CdS surface were optimized. A H_2 evolution rate up to 1224 $\mu mol \cdot h^{-1}$ has been achieved for the 9.6 mol% ZnS–1 mol% WS_2/CdS photocatalyst. The enhancement of the photocatalytic activity is attributed to the synergistic effect of WS_2 as co-catalyst and ZnS as passivation layer.

1. Introduction

Photocatalytic H_2 generation from water has attracted increasing attention recently [1–3]. In order to utilize the abundant visible light, developing visible light driven photocatalysts is indispensable. Sulfide photocatalysts (such as $CuInS_2$ [4], CdS [5], $ZnIn_2S_4$ [6], etc.) are generally attractive candidates due to their suitable band gaps and good catalytic activities for H_2 evolution. In particular, CdS is widely studied as an important sulfide for its suitable band positions as well as its low cost. However, its photocatalytic efficiency is extremely low due to severe recombination, and it's not stable under irradiation due to photocorrosion.

Generally, the above problems can be greatly solved by loading noble metals or their oxides (such as Pt, Pd, RuO_2, etc.) as co-catalysts, which facilitate the separation of photo-generated electrons and holes and afford the redox reaction sites [7–9]. However, the noble metals are not appropriate for practical application. In order to reduce the cost, some metal sulfides as co-catalysts, such as MoS_2 [10], WS_2 [11] and NiS [12], have been recently reported to replace noble metals. In the meantime, for the CdS nanoparticles, some photo-generated carriers are easily captured by its surface states, surface passivation is thus supposed to be a good modification method to restrain this surface trapping. In quantum-dot sensitized solar cells, ZnS passivation layer has been widely used to reduce electron losses of quantum dot sensitizers. That is to say, some surface states of CdS can be passivated by ZnS with higher conduction band and lower valence band, which is further favorable for the photocatalytic reaction [13–15].

Herein, we report a novel noble metal-free ZnS–WS_2/CdS composite photocatalyst for H_2 evolution, which is obtained by our recently developed ball-milling (BM) combined calcination method for WS_2 loading [16] and subsequently hydrothermal treatment for ZnS loading on CdS. A H_2 evolution rate up to 1224 $\mu mol \cdot h^{-1}$ has been achieved for the 9.6 mol% ZnS–1 mol% WS_2/CdS photocatalyst. The synergistic effect of ZnS as passivation layer and WS_2 as co-catalyst is supposed to contribute to the increase of the photocatalytic activity.

2. Experimental

2.1. Photocatalyst preparation

CdS powder was from Beijing Shuanghuanweiye Reagent Co., Ltd. $Zn(Ac)_2 \cdot 2H_2O$, thiourea and lactic acid were from Sinopharm Chemical Reagent Co., Ltd. All the chemicals were analytical grade (AR) and used directly except for the CdS which was thermally treated in advance [16–18]. The $(NH_4)_2WS_4$ was synthesized according to the literature (details in Supporting Information) [19].

---

* Correspondence to: D. Li, Key Laboratory for Renewable Energy, Institute of Physics, Chinese Academy of Sciences, Beijing 100190, PR China. Tel./fax: +86 10 82649242.
** Correspondence to: Q. Meng, Key Laboratory for Renewable Energy, Institute of Physics, Chinese Academy of Sciences, Beijing 100190, PR China. Tel./fax: +86 10 82649242.
E-mail addresses: dmli@iphy.ac.cn (D. Li), qbmeng@iphy.ac.cn (Q. Meng).

http://dx.doi.org/10.1016/j.catcom.2013.05.025

The WS_2/CdS photocatalysts with different WS_2 loading amounts (denoted as *x* mol% WS_2/CdS) were prepared by our recently developed ball-milling combined calcination method (details in Supporting Information) [16]. ZnS was then loaded on the 1 mol% WS_2/CdS as follows: the slurry containing a proper amount of $Zn(Ac)_2 \cdot 2H_2O$, 10 mmol of thiourea, 0.3 g of as-prepared 1 mol% WS_2/CdS (treated at 723 K) and 35 mL deionized H_2O was ultra-sonicated for 1 h, then transferred into a Teflon-lined autoclave and maintained at 393 K for 5 h. The ultimate solids (denoted as *y* mol% ZnS–1 mol% WS_2/CdS) were collected by centrifugation and washing with distilled water for several times. Here, *x* or *y* means the loading molar quantity of ZnS or WS_2 per 100 mol CdS. For comparison, the 1 mol% WS_2–9.6 mol% ZnS/CdS photocatalyst and the 9.6 mol% ZnS/CdS photocatalyst were also prepared by the same method.

2.2. Characterization

The surface morphologies were obtained by a scanning electron microscope (SEM, XL30 S-FEG, FEI) and a transmission electron microscope (TEM, JEM-2010, JEOL Ltd.). The X-ray diffraction (XRD) patterns were collected by a rotating-anode diffractometer with Cu K_α radiation (M18X-AHF, MacScience). The X-ray photoelectron spectra (XPS) were recorded on an ULVAC-PHI X-ray photoelectron spectrometer (PHI Quantera SXM) using Al K_α radiation. The thermal decomposition behavior was studied by a differential thermal analysis/thermogravimetric analysis instrument (DTA/TGA, NETZSCH STA 449F3) in N_2 atmosphere with the heating rate of 10 K/min. The photoluminescence spectra were recorded on an FLS 920 fluorescence spectrometer (Edinburgh Instruments).

2.3. Photocatalytic performance

The reaction was performed in a Pyrex reaction cell connected to a closed gas circulation and evacuation system. 0.1 g photocatalyst powder was dispersed in a 150 mL aqueous solution containing 15 mL lactic acid as the sacrificial reagent [12]. The suspension was irradiated by a 300 W Xenon lamp equipped with an optical cut-off filter ($\lambda > 420$ nm). The temperature of the reaction solution was maintained at 293 ± 1.5 K by a cooling liquid flow. The evolved H_2 amount was determined by an on-line gas chromatography. The photocatalytic activities were compared by the average H_2 evolution rate in the first 5 h.

3. Results and discussion

The XRD patterns of the WS_2/CdS photocatalysts treated at different temperatures indicate that CdS always keeps the hexagonal phase during the thermal treatment (see Fig. 1(a)), whereas diffraction peaks assigned to WS_2 are not observed due to low loading amount. The TG–DSC curve of $(NH_4)_2WS_4$ and XRD patterns of different temperatures treated $(NH_4)_2WS_4$ confirm that $(NH_4)_2WS_4$ is completely decomposed into WS_2 above 673 K (see Fig. S1 and Fig. 1(b)). This is also validated by XPS spectra (see Fig. 1(c)). The W4f peaks at 35.7 and 37.9 eV are assigned to W^{6+} while the peaks at 32.6 and 34.8 eV can be assigned to W^{4+} in WS_2 [20].

For 1 mol% WS_2/CdS photocatalysts, the influence of calcination temperature on H_2 evolution rate was firstly investigated. As illustrated in Fig. 2(a), with the temperature increasing, the H_2 evolution rate of 1 mol% WS_2/CdS increases gradually, reaching the maximum value of 780 $\mu mol \cdot h^{-1}$ at 723 K. However, further increasing the temperature will decrease the H_2 evolution rate instead, which may be ascribed to the decrease of the surface areas. From SEM images of 1 mol% WS_2/CdS samples calcined at different temperatures, we can see that with the temperature increasing, the particle sizes increase gradually. It is supposed that some small particles grow together into larger ones, as shown in Fig. S2.

Fig. 2(b) shows the H_2 evolution rates of WS_2/CdS photocatalysts with different WS_2 amounts. The H_2 evolution rate of bare CdS is only 85 $\mu mol \cdot h^{-1}$. After loading 0.25 mol% WS_2, the H_2 evolution rate increases sharply to 262 $\mu mol \cdot h^{-1}$. With 1 mol% WS_2 loaded, the H_2 evolution rate reaches the maximum of 780 $\mu mol \cdot h^{-1}$, which is much higher than 488 $\mu mol \cdot h^{-1}$ for 0.2 wt.% Pt/CdS photocatalyst [16,17]. However, further increasing the WS_2 amount results in the decrease of the H_2 evolution rate, possibly due to the introduction of recombination sites and the light shading effect of WS_2 [16].

In order to further improve the photocatalytic activity, ZnS was loaded on WS_2/CdS photocatalysts. As shown in Fig. 2(c), with the increase of the ZnS amount, the H_2 evolution rate increases firstly, reaching the maximum of 1224 $\mu mol \cdot h^{-1}$ for 9.6 mol%, then decreases gradually due to the incident light hinder and the introduction of recombination centers by excessive ZnS. For comparison, a H_2 evolution rate of 104 $\mu mol \cdot h^{-1}$ is obtained for the 9.6 mol% ZnS/CdS photocatalyst, slightly higher than that of the bare CdS whereas far lower than the ZnS–WS_2/CdS photocatalysts. Obviously, the loadings of WS_2 and sequent ZnS are simultaneously beneficial to improve the photocatalytic activity.

Fig. 3(a) and (b) clearly shows that WS_2 with a typical layered structure is deposited on the surface of CdS, depicted by the black circles, of which the lattice spacing of the (002) plane is 6.18 Å. As shown in Fig. S3, some small ZnS particles are dispersed at the CdS nanoparticle surface after hydrothermal treatment. The HRTEM images (Fig. 3(c) and (d)) demonstrate the small particles are ZnS for the lattice spacing of 3.3 Å is (100) planes (depicted by the white circles).

As we know, the photoluminescence (PL) spectroscopy is an effective way to investigate the photo-generated charge transfer and recombination processes. Herein, at the excitation wavelength of 400 nm, the PL spectra are presented in Fig. 4. The CdS sample displays the highest emission band intensity centered at 700 nm, which is ascribed to the trap-related states that generally serve as recombination centers. As

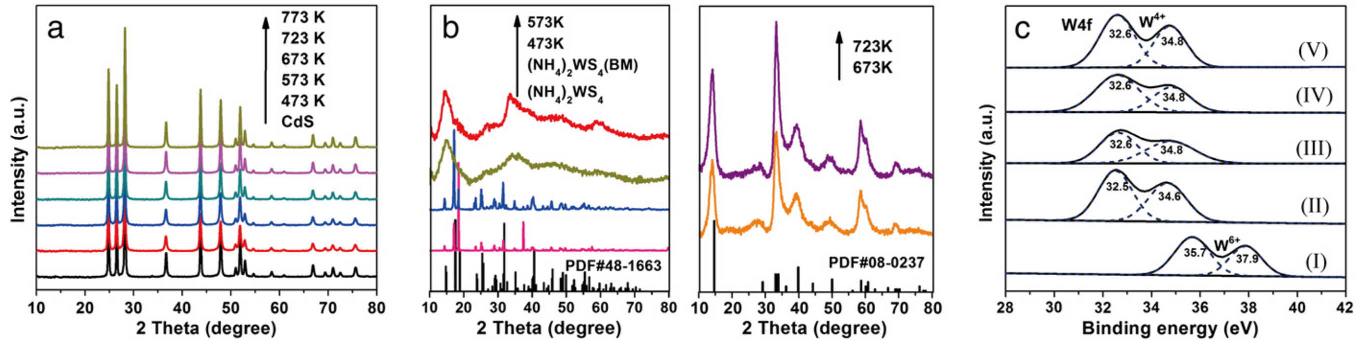

Fig. 1. (a) X-ray diffraction patterns of 1 mol% WS_2/CdS photocatalysts calcined at different temperatures, along with thermally treated CdS for comparison; (b) X-ray diffraction patterns of $(NH_4)_2WS_4$, $(NH_4)_2WS_4$ (BM), and WS_2 prepared by calcining $(NH_4)_2WS_4$ (BM) at different temperatures; and (c) XPS spectra of the W4f regions for 1 mol% WS_2/CdS photocatalysts prepared at (I) 573 K, (II) 673 K, (III) 723 K, (IV) 773 K and (V) 9.6 mol% ZnS–1 mol% WS_2/CdS photocatalyst.